

# Crystallization Kinetics of Palm Oil

K.P.A.M. van Putte and B.H. Bakker

Unilever Research Laboratorium Vlaardingen, P.O. Box 114, 3130 AC Vlaardingen, The Netherlands

The quality and yield of oils obtained by fractionation processes depend mainly on the separation efficiency of fat crystals from the mother liquor; this process is, to a large extent, determined by crystal-size distributions. The size of the crystals is influenced by the crystallization conditions applied, and the quantitative data on crystallization kinetics are a useful tool to optimize and control such a process. The crystallization work described concerns the fractionation of edible oils and fats. Palm oil was chosen as a model system.

We quantified the growth and primary nucleation rates of saturated crystals in palm oil. The growth rate was proportional to the degree of supersaturation of the oil component studied, suggesting that the screw dislocation mechanism as described by Burton, Cabrera and Frank is determinative of the growth rate. Also the primary nucleation rate depends on the degree of supersaturation and can be described by the Becker and Döring equation. Special attention was paid to the experimental setup, which enabled us to measure the rate constants of both mechanisms separately. The kinetic data obtained were used to predict solid phase curves. The agreement between measured and predicted solid phase curves is satisfactory and in conformity with our model description. The results of our experiments also show that the crystallization kinetics of oils and fats can be described by the equations often used for inorganic systems.

The fractionation of edible fats is a modification process becoming increasingly important in food processing. Edible fats are complex multicomponent mixtures of different triacylglycerols with different melting points. The melting behavior and/or the clear point of fats are important properties when used in margarines, table oils or specialty fats.

Fractionation separates fats into fractions with different melting properties. This process is based on the crystallization of part of the fat, followed by a separation of the crystals from the mother liquor. Crystallization from a cooled melt or from a solution using an organic solvent is applied commercially. Separation of crystals is often difficult and far from complete, especially from a melt. This problem is attributable to small-sized crystals retaining a relatively large amount of mother liquor. The size of the crystals may vary considerably (1-1,000  $\mu\text{m}$ ) and is determined by the crystallization conditions applied.

To describe the crystal-size distributions, it is necessary to know rate constants of the following processes: nucleation, growth, agglomeration and attrition. Unfortunately, little is known about the rate constants of edible fats, probably because of their complex composition and morphology. Part of these kinetic data relate to simple pure systems (1). A recent model study provided crystallization data for hydrogenated soybean oil (2).

TABLE 1

Analytical Data of the Palm Oil (PO) Fractions Used in This Study

		Refined PO	Topped PO
Iodine value		53.6	
Diacylglycerols (%) by HPLC		7.4	5.7
Triacylglycerols (%)		92.6	94.3
Peroxide value		3.9	
Free fatty acids (%)		0.12	
Water (%)		0.03	
Fatty acid composition (%)			
	C14:0	1.0	
	C16:0	43.7	
	C18:0	4.7	
	C18:1	39.1	
	C18:2	10.5	
	C18:3	0.2	
	C20:0	0.4	
Diacylglycerols composition (%) by HPLC			
	1.3	5.3	3.9
	1.2	2.1	1.8
Triacylglycerols composition (%) by HPLC			
	SSS	8.8	1.65
	SOS	34.5	34.6
	SLS/SSL	10.3	9.3
	SOO	23.7	31.7
	SLO/OOO	12.8	18.6
	OLO/OOL	3.8	
	LOL/LLO	-	

S, saturated; O, oleoyl; L, linoleoyl.

In this study the so-called mixed-suspension, mixed-product removal crystallizer was used; agglomeration and attrition were assumed to be negligible, but agglomeration often plays an important role during the crystallization of edible fats in stirred vessels (3).

In the present study, the growth and primary nucleation rate of palm oil crystals have been measured in a batch crystallizer at non-stirring conditions, thus avoiding secondary nucleation. Special attention was paid to the experimental setup, enabling us to measure the rate constants of both mechanisms separately. For the description of these mechanisms we used the same type of equations as for inorganic crystallization processes. Crystal-size distributions were calculated using the population balance approach, and the assumptions made were checked.

## MATERIALS AND METHODS

Palm oil was chosen as a model system. Table 1 gives some analytical data of the fractions used in this study: neutralized and bleached palm oil, and palm oil topped at 22 C. The fractions are referred to as refined palm oil and topped palm oil, respectively. The trisaturated triacylglycerol content was 8.8% for refined palm oil and 1.65% for topped palm oil.

## CRYSTALLIZATION KINETICS OF PALM OIL

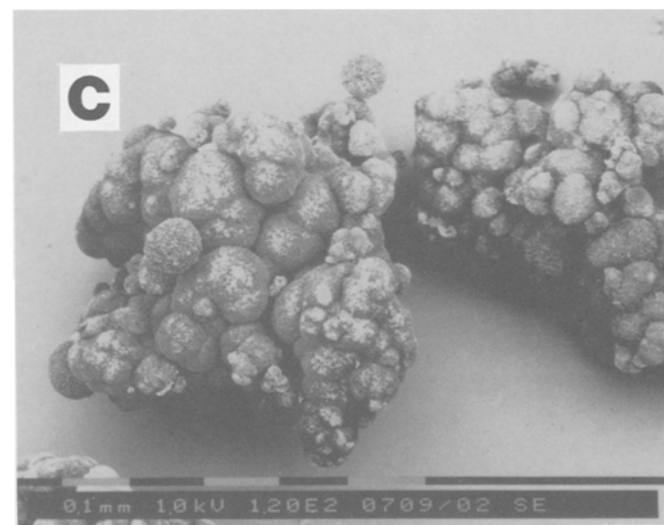
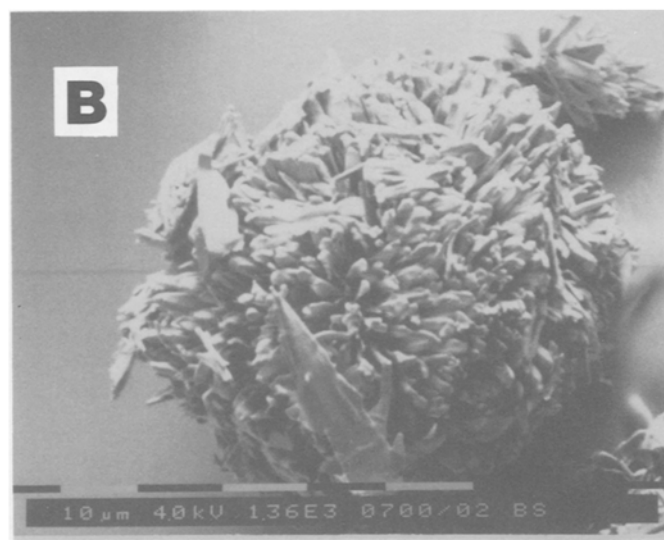
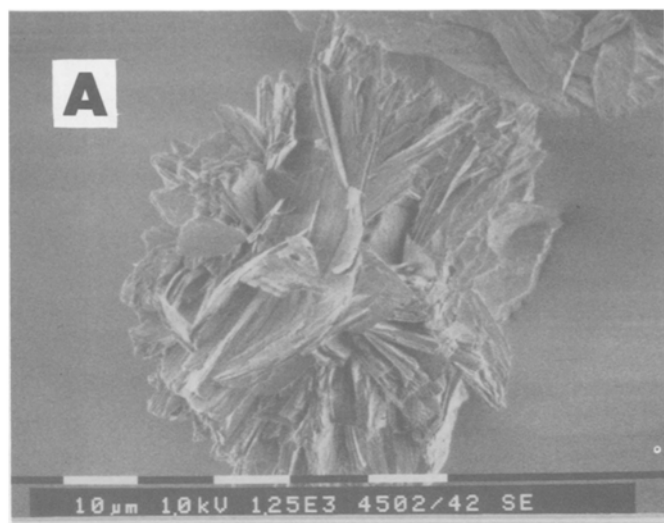


FIG. 1. Electron photomicrographs of the polymorphic forms of palm oil SSS crystals. A,  $\beta$  (non-stirred); B,  $\beta'$  (non-stirred); C,  $\beta'$  (agglomerated).

**Crystal-size distribution.** The crystal-size distribution was measured with a Malvern ST 1800 particle-size analyzer. The technique is based on laser light diffraction by spherical particles (5). The density of the crystals in part of the samples was so high that dilution with crystal-free refined palm oil was necessary. This palm oil was obtained by heating the oil at 70 C and subsequently cooling down to the measuring temperature. The oil remained clear for more than one hr (induction period). The amount of solids should not exceed 0.1%.

The Malvern analyzer was connected to a computer for performing fitting procedures. The crystal-size distributions could be approximated satisfactorily by superposition of the log normal distributions of the large and small crystals, respectively.

**Growth rate measurement.** The growth rate of the  $\beta$ -modification of trisaturated triacylglycerols (SSS) of palm oil was measured between 34 and 46 C. Refined palm oil was nucleated at 31 C in a one-l vessel for 30 min. After this period, the palm oil is still clear although it contains small crystals. To obtain a narrow initial size distribution, the temperature was quickly raised to 39 C, causing the smallest nuclei to melt. Further narrowing of the crystal-size distribution was achieved by filtering part of the oil through a 5- $\mu\text{m}$  filter medium.

Approximately 50 g of filtrate was added to a second vessel together with about one l of nuclei-free palm oil brought to the growth rate measuring temperature. After mixing, stirring was discontinued to avoid secondary nucleation. Subsequently, the crystal-size distribution was measured with the Malvern particle-size analyzer as a function of time. The crystal growth rate was calculated by plotting the crystal size at maximum peak height (mode) of the weight frequency distribution versus time.

The growth rate of the  $\beta'$ -modification of SSS crystals in topped palm oil was measured similarly between 21 and 29 C.

**Nucleation rate measurement.** Primary nucleation rates of the  $\beta'$ -modification of palm oil SS crystals were measured in non-agitated glass tubes with a diameter of 10 mm. A number of tubes were filled with approximately 3 g of oil and heated to 70 C for at least 30 min. Subsequently, the tubes were placed in a thermostatted bath at the temperature desired.

A small amount of oil was taken from the tube and

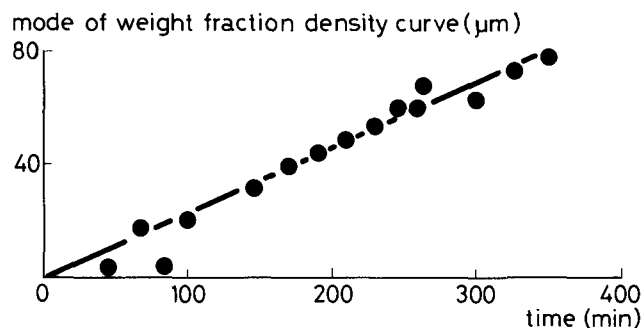


FIG. 2. Growth rate of refined palm oil SSS  $\beta$ -crystals at 39 C ( $G = 13.9 \mu\text{m/hr}$ ).

introduced into a Fuchs-Rosenthal counting cell. The depth of the cell was 100  $\mu\text{m}$ . The temperature of the cell was kept at 30 and 40 C for the systems with 1.65 and 8.8% SSS. Due to the relatively high temperature, the nucleation rate is low during counting. The number of crystals present in a well-defined volume of oil of  $2.5 \times 10^{-11} \text{ m}^3$  was counted using a Zeiss microscope (magnification 100 $\times$ ). In one sample, 10-20 counts were done of which the mean value was calculated. A new sample was taken from a second tube to avoid secondary nucleation by cumulative agitation of the oil. The primary nucleation rate was determined by plotting the mean value of the counts as a function of time.

The nucleation rate of the  $\beta$ -modification is considerably lower than that of the  $\beta'$ -modification. Moreover, the distribution of the crystals over the sample was often far from homogeneous, and the accuracy of these counting experiments was, therefore, relatively poor.

**Population balance approach.** The nucleation and growth rate data obtained were used to calculate the crystal-size distribution and the solid phase curve. For this purpose, we used the so-called population balance approach (4) obtained from the balance equations over all generated and disappearing crystals. We reckoned with nucleation and growth effects but neglected agglomeration and attrition contributions. This approach gave the following simplified population balance equation:

$$\frac{\delta n}{\delta t} + \frac{\delta(GN)}{\delta D} = 0 \quad [1]$$

where:  $G$  = growth rate ( $\mu\text{m/hr}$ )  
 $D$  = diameter ( $\mu\text{m}$ )  
 $t$  = time (hr)  
 $n = dN(t)/dD =$  density number/ $\text{m}^3$  with diameter between  $D$  and  $D + dD$   
 $N(t) = \int_0^D n dD =$  total number of particles/ $\text{m}^3$  with sizes smaller than  $D$

Equation [1] is a first-order partial differential equation with time- and size-dependent coefficients. It was solved numerically at the University of Technology in Delft, The Netherlands (6). A special computer program was written for it, known as the fraction-trajectory model.

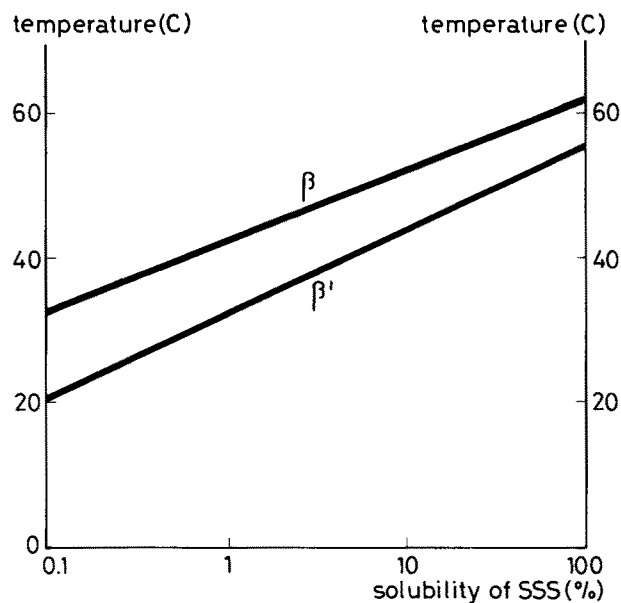


FIG. 3. Solubility of SSS in palm oil.

In this fraction-trajectory model, equation [1] was reduced to two normal differential equations by separately calculating the influence of crystal growth and nucleation on the crystal-size distribution. This was done by calculating the number of crystals during growth at distinct size intervals. Nucleation was taken into account by calculating the number of nuclei generated during the time increment  $dt$ . This number of nuclei was stored in a new size interval. The size of the nuclei was neglected.

## RESULTS AND DISCUSSION

**Spherulitic growth.** The shape of triacylglycerol crystals formed at relatively high super-cooling is often spherulitic (1). Figures 1A and 1B show electron photomicrographs of the polymorphic forms,  $\beta$  and  $\beta'$ , of saturated palm oil fraction crystals, which consist mainly of SSS. The triacylglycerol composition of several samples of crystals was determined (after filtering and washing the crystals) by HPLC. The amount of trisaturated compound was more than 75% for the crystals at

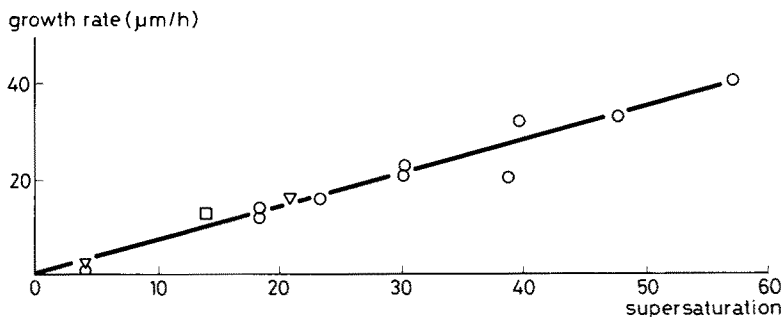


FIG. 4. Growth rate of palm oil SSS  $\beta$ -crystals as a function of supersaturation,  $\sigma$  ( $G = 0.70 \sigma \mu\text{m/hr}$ ).  $\circ$ , palm oil with 8.8% SSS;  $\diamond$ , palm oil with 12.8% SSS;  $\square$ , microscopic observation.

## CRYSTALLIZATION KINETICS OF PALM OIL

34-46 C and more than 55% for the crystals at 21-29 C. These observations, combined with the X-ray diffraction data, indicate that the main components, crystallizing at 34-46 C and 21-29 C, are  $\beta$ -SSS and  $\beta'$ -SSS, respectively.  $\beta'$ -spherulites consist of numerous needles growing from the center of the spherulites, whereas  $\beta$ -spherulites have a more platelike structure.

The crystals shown in Figures 1A and 1B were obtained under non-stirring conditions. Figure 1C is a typical example of agglomerates of  $\beta'$ -crystals obtained under stirring conditions. Often, agglomeration will increase the mean particle size considerably as soon as stirring is applied (3).

**Growth rate.** The crystal size distributions measured with the Malvern particle size analyzer showed two peaks. The peak corresponding to the largest crystals shifted to larger sizes at increasing time intervals due to growth, whereas the position of the peak relating to the smallest crystals remained almost constant. Small crystals are attributable to a slow nucleation in the bulk liquid, which was cooled down to the measuring temperature just before the filtered crystal slurry was added. The weight fraction of these small crystals

varied in relation to the crystallization time but did not exceed 30%.

Figure 2 is a typical plot of the peak of the large crystals versus time. The size at maximum peak height increases linearly with time, indicating the growth rate to be size-independent: the time-independent peak width points in the same direction. The growth rate of SSS  $\beta$ -crystals in refined palm oil is 13.9  $\mu\text{m/hr}$  at 39 C.

The growth rate depends greatly on temperature because of the temperature dependence of supersaturation, which is the driving force of growth. The supersaturation  $\sigma$  is defined as:

$$\sigma = \frac{c - c^*}{c^*} \quad [2]$$

where:  $c$  = actual concentration  
 $c^*$  = saturation concentration

The supersaturation was calculated on the basis of HPLC data for the SSS content, assuming the growth rate of the (mixed) crystals to be controlled by these triacylglycerols. The saturation concentrations were derived from solubility curves (Fig. 3), which were obtained by measuring the clear points of several topped palm oil compositions.

Figure 4 shows the relationship between growth rate and supersaturation to be linear for the  $\beta$ -polymorphic form:  $G = 0.70 \sigma \mu\text{m/hr}$ . We investigated two types of palm oil with strongly differing SSS contents (Fig. 4); both types satisfactorily fit this growth model equation.

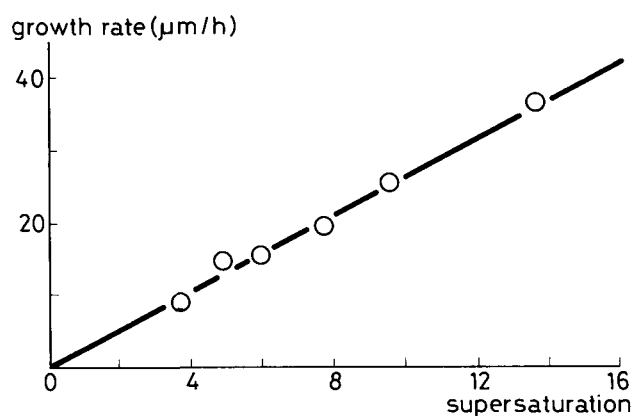


FIG. 5. Growth rate of SSS  $\beta'$ -crystals in topped palm oil as a function of supersaturation,  $\sigma$  ( $G = 2.7 \times \sigma \mu\text{m/hr}$ ).

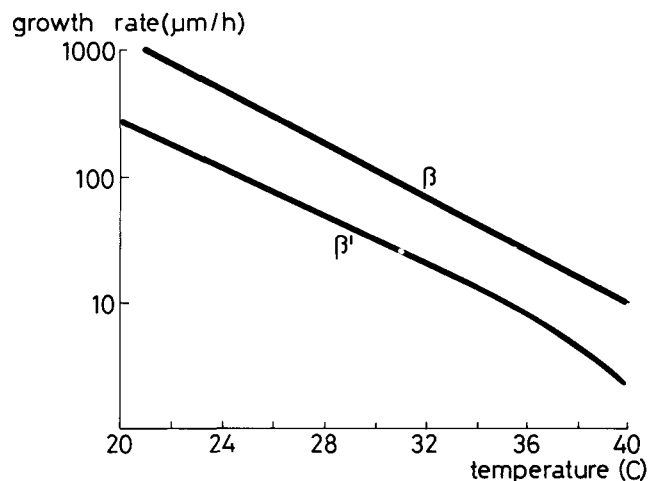


FIG. 6. Growth rate of SSS  $\beta$ - and  $\beta'$ -crystals in refined palm oil as a function of temperature.

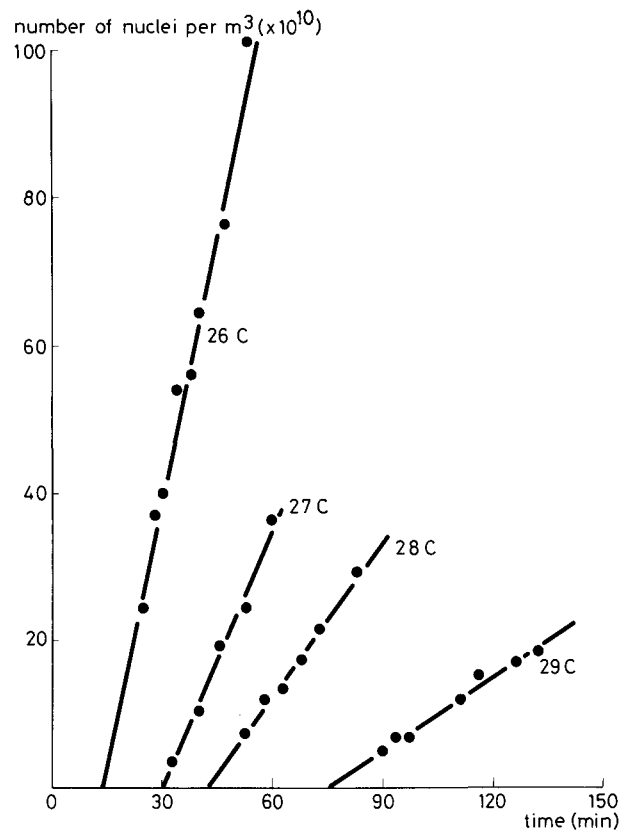


FIG. 7. Primary nucleation rate measurements of  $\beta'$ -SSS crystals in refined palm oil.

In addition to the measurements with the Malvern analyzer, we followed the growth of a single crystal with the microscope. The measured growth rate (Fig. 4) was in good agreement with the Malvern values.

The growth rate of the  $\beta'$ -polymorphic form was measured in topped palm oil and not in refined palm oil because of its high growth and nucleation rates. The  $\beta'$ -polymorphic form remained stable for at least 4 hr in the temperature range 21 to 28 C. The growth rate constant of the  $\beta'$ -polymorphic form (2.7  $\mu\text{m/hr}$ ) proved to be about four times higher than that of the  $\beta$ -polymorphic form (Fig. 5). The linear relationship between growth rate and supersaturation is in accordance with the screw dislocation mechanism described by Burton et al. (7).

We also calculated the growth rate of the  $\beta$ - and  $\beta'$ -polymorphic forms in refined palm oil between 20 and 40 C, using the growth rate equations mentioned above (Fig. 6). The growth rate of the  $\beta$ -polymorphic form is high compared with that of the  $\beta'$ -polymorphic form despite its lower growth rate constant. This can be ascribed to the relatively high supersaturation (low solubility) of the  $\beta$ -form.

**Primary nucleation rate.** Primary nucleation can be described as an ordering process in solution. As soon as a cluster of molecules in the solution has grown to a certain critical size, intermolecular forces within the

cluster start prevailing over the forces of the nearest molecules in the surrounding solution. Consequently, the cluster becomes stable and forms a crystal nucleus. For the primary nucleation rate ( $B_{op}$ ) Becker and Döring (8) derived the following Arrhenius-type equation:

$$B_{op} = k_{np} 10^{-A_{np}/\{\log(\sigma+1)\}^2} \quad [3]$$

where  $k_{np}$  and  $A_{np}$  are primary nucleation constants.

We measured the primary nucleation rate of the  $\beta'$ -polymorphic form of SSS in palm oil by counting the number of crystals. The amount of solids formed during our experiments was smaller than 0.1%, and the supersaturation—and therefore the primary nucleation rate (see eq. 3)—can be considered constant. Figure 7 shows that the number of nuclei per unit of volume increases linearly with time, which means that the nucleation rate represented by the slope of the line is indeed time independent as long as the degree of supersaturation remains constant.

During the so-called induction period, represented by the intercept in Figure 7, no crystals were observed, because of their limited number and small size (9).

The slopes of the lines in Figure 7 strongly depend on temperature. The nucleation rate decreases rapidly with increasing temperature. The temperature-dependent supersaturation is the driving force of nucleation (eq. 3), and we therefore plotted (on a logarithmic scale) the nucleation rate as a function of the supersaturation term in equation 3,  $1/\{\log(\sigma+1)\}^2$  (Fig. 8). This relationship is linear for both polymorphic forms of SSS palm oil.

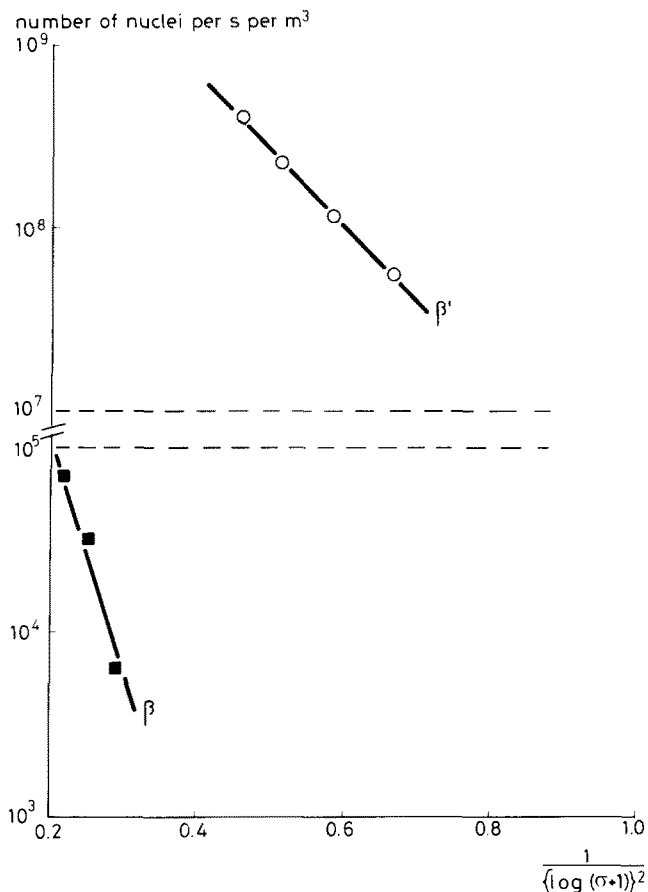


FIG. 8. Primary nucleation rate of SSS  $\beta$ - and  $\beta'$ -crystals in palm oil as a function of supersaturation.  $\beta'$ :  $k_{np} = 10^{10.40}$ ,  $A_{np} = 3.98$ ;  $\beta$ :  $k_{np} = 10^{7.76}$ ,  $A_{np} = 13.48$ .

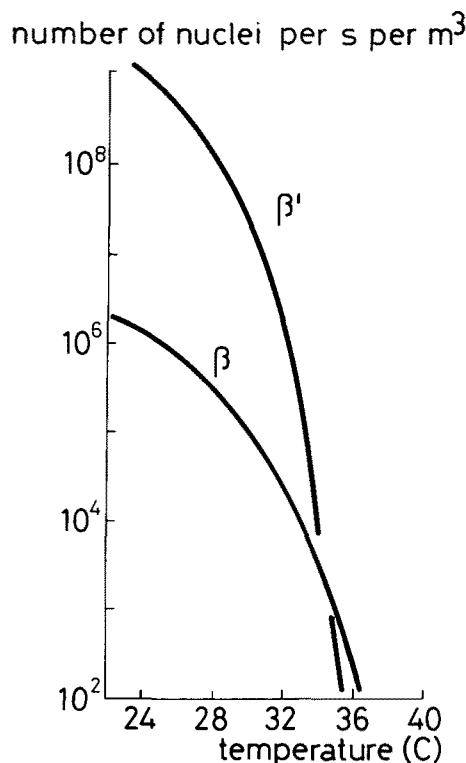


FIG. 9. Primary nucleation rate of SSS  $\beta$ - and  $\beta'$ -crystals in refined palm oil as a function of temperature.

## CRYSTALLIZATION KINETICS OF PALM OIL

The constants  $A_{np}$  and  $k_{np}$  of equation 3 can be calculated from the slope and the intercept with the vertical axis, respectively. The calculated constants  $k_{np}$  and  $A_{np}$  for the  $\beta'$ -polymorphic form of SSS in refined palm oil were  $10^{10.40}$  and 3.98, respectively, and for the  $\beta$ -polymorphic form  $10^{7.76}$  and 13.48.

On the basis of these data, we recalculated the primary nucleation rate in palm oil as a function of temperature for both polymorphic forms (Fig. 9). The primary nucleation rate of the  $\beta'$ -polymorphic form is fast compared with that of the  $\beta$ -polymorphic form below 35 C.

*Calculation of solid phase curve.* We checked the assumptions made and the kinetic data obtained so far by calculating crystal-size distributions and solid phase curves of palm oil under non-stirring conditions using the fraction-trajectory model. Figure 10 shows typical crystal-size distributions during crystallization of  $\beta'$ -modification at 28 C. The weight density is normalized, so the total area under the weight density curve equals unity.

By this procedure, the crystal size-distribution is computed after a small time increment while the degree of supersaturation is kept constant. After each time increment, the supersaturation is recalculated from the amount of solids crystallized. However, it should be noted that supersaturation was defined in relation to the pure SSS component, whereas the solids consist of mixed crystals. The SSS content of the crystals varied considerably (from about 60 to 80%) which, however, seemed to have a negligible effect on growth and nucleation rates. The supersaturation with respect to the pure component was related to the solids content in the actual system using the following overall equation for the fraction (F) of SSS in the mixed crystals:

$$F = \frac{S_{SSS} - S^*}{S_e} \quad [4]$$

where  $S_e$  = fraction of solids at equilibrium conditions

$S^*$  = fraction of SSS dissolved

$S_{SSS}$  = fraction of SSS in palm oil

The conversion factor represents the fraction of SSS in the mixed crystals.

Figure 11 shows the predicted and measured solid phase curves of refined palm oil at 26, 27 and 28 C; the data are in good agreement, indicating that our model description is correct. The growth and nucleation rates determined independently during the onset of crystallization (at  $\sim 0.1\%$  solids) can be used to predict quantitatively the whole curve including the induction period.

The simplification made in our model to regard crystals as completely solidified spheres proves to be sound.

## REFERENCES

1. Skoda, W., and M. van der Tempel, *J. Cryst. Growth* 1:207 (1967).

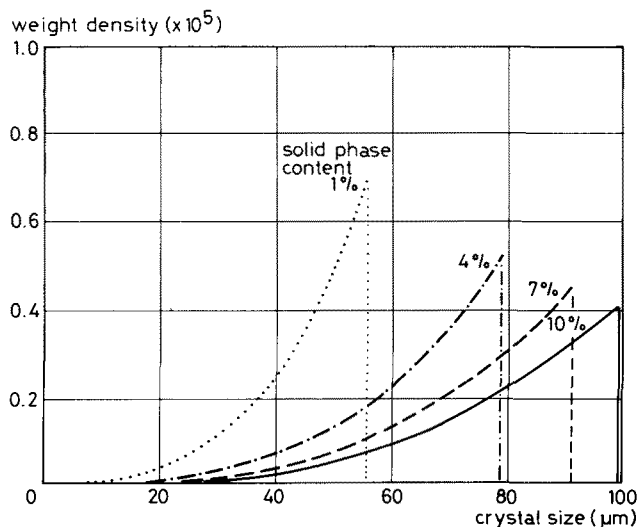


FIG. 10. Crystal-size distribution of SSS  $\beta'$ -crystals at 28 C and at different solid phase contents.

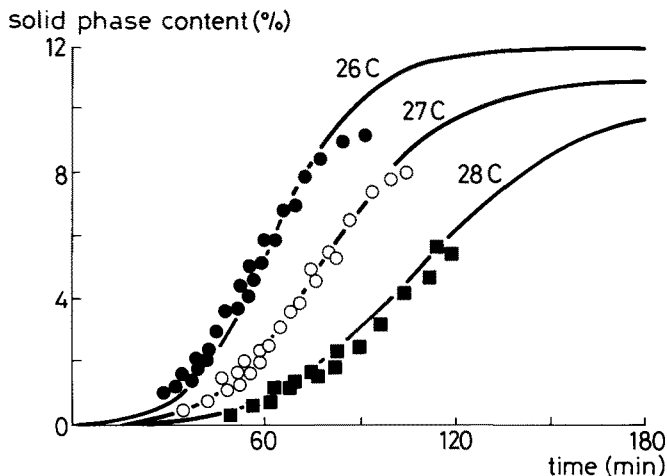


FIG. 11. Calculated (line) and measured (symbols) solid phase curves of refined palm oil.

2. Singh, G., *AICHE Symp. Ser. no 153* 72:100 (1976).
3. Bemer, G.G., and G. Smits, *Proc. 2nd World Congress of Chemical Engineering*, Montreal, Canada, I, pp. 369-371 (1981).
4. Randolph, A.D., *Industrial Crystallization* 78:295 (1979).
5. Weiner, B.B., *Soc. of Photo-Optical Instrumentation Engineers* 170:53 (1979).
6. De Leer, B.G.M., Ph. D. Thesis, University of Technology, Delft, The Netherlands, November 1981.
7. Burton, W.K., N. Cabrera and F.C. Frank, *Nature* 163:398 (1949).
8. Becker, R.R., and W. Döring, *Ann. Physik* 24:719 (1935).
9. Khamskii, E.V., *Crystallization from Solutions*, Consultants Bureau, New York - London, 1969.

[Received August 15, 1986]